

Cl incorporation into successively zoned amphiboles from the Ramnes cauldron, Norway

HISAO SATO,* YOSHIAKI YAMAGUCHI, AND KUNIAKI MAKINO

Department of Geology, Faculty of Science, Shinshu University, Asahi, Matsumoto 390, Japan

ABSTRACT

Amphibole from alkali granites in the Ramnes cauldron in the Oslo rift was altered hydrothermally by corrosion and growth through multiple events of fluid circulation. The alteration developed successive zones of amphibole at the crystal margins, resulting in a (1) brownish ferro-edenitic hornblende core (FE), (2) deep bluish-green hastingsitic hornblende zone (HH), and (3) light-greenish Fe-rich actinolite rim (FA). The edenitic core preserves the original igneous amphibole composition. The Cl content of amphibole strongly increases from the FE (0.78–0.82 wt%) to the HH zone (2.07–2.96 wt%) and abruptly decreases in the FA rim (0.01–0.36 wt%). In the Cl-rich HH amphibole zone, amphibole has characteristically high Cl content [2.96 wt%, 0.82 atoms per formula unit (apfu)] and high concentrations in both ^{141}Al (1.73 apfu) and A-site occupancy (0.86 apfu) with a large $\text{K}/(\text{Na} + \text{K})$ value of 0.47.

Both ^{141}Al and A-site occupancy increase systematically with positive correlation with Cl content throughout the three amphibole zones. On the other hand, Fe^{2+} content is not so simply correlated to the Cl content. Based on crystal structure considerations on Cl-rich amphiboles, the cation substitutions are illustrated by structural (geometrical) constraints for ^{141}Al and by a chemical constraint for Fe^{2+} . These contributions for Cl incorporation are expressed empirically by $\ln(\text{Cl}/\text{OH})_{\text{amp}} = \ln(\text{Cl}/\text{OH})_{\text{fluid}} + A \cdot ^{141}\text{Al} \cdot \text{Fe}^{2+}/RT + B/RT$, where A and B are constant. $^{141}\text{Al} \cdot \text{Fe}^{2+}$ vs. $\ln(\text{Cl}/\text{OH})$ plots of the three distinct amphibole zones suggest different fluid conditions in chemistry and temperature for the three zones. The zoning was developed through two stages of hydrothermal alteration. In the early hydrothermal event, a saline and high-temperature fluid altered the original hornblende (FE) to the Cl-rich HH zone. Late stage alteration by a high Fe/Cl and relatively low-temperature fluid partially over-printed the FA zone at the crystal margin.

INTRODUCTION

Cl in magma and the post-magmatic fluids plays an important role in devolatilization of magma, hydrothermal alteration, and ore genesis. Cl is strongly partitioned into fluid relative to coexisting melt or solid phases and can affect the solubility of specific metals and transport them as metal-chloride complex in hydrothermal fluids (Kilinc and Burnham 1972; Burnham and Ohmoto 1980; Shinohara et al. 1989). The Cl content of hydrous minerals such as amphibole, mica, and apatite is expected to reflect coexisting fluid composition (Nedachi 1980; Chivas 1981; Munoz 1984; Vanko 1986; Morrison 1991; Enami et al. 1992). Cl-rich amphiboles ($\text{Cl} \geq 1.5$ wt%) have been described from hydrothermally altered rocks and metamorphic rocks (Dick and Robinson 1979; Ito and Anderson 1983; Vanko 1986; Suwa et al. 1987; Morrison 1991; Enami et al. 1992).

On account of the larger ionic radius of Cl relative to

those of OH and F, previous reports have focused on the correlations between Cl incorporation and the cationic substitutions in amphiboles. Volfinger et al. (1985) suggested a large structural effect on expansion of the octahedral strip by substitution of Cl for the hydroxyl sites in micas and also amphiboles. Ito and Anderson (1983) and Suwa et al. (1987) indicated that Cl content in amphiboles is correlated positively with the contents of Al in tetrahedral sites and Fe^{2+} in octahedral sites. Vanko (1986) suggested that structural controls between Cl incorporation and Fe substitution into octahedral sites are not effective, but Cl content of amphibole varies as a function of the Cl activity of the coexisting hydrothermal fluid. Enami et al. (1992) argued that the Cl content of amphibole increases with increasing chlorinity of the coexisting fluid in Cl-poor environments, but that on the other hand, the crystal-chemical controls become more important in the Cl-rich fluid conditions of the Salton Sea geothermal system. There the Cl content strongly depends on octahedral Fe^{2+} and A-site occupancy.

Morrison (1991) found a relatively large Mg-Cl avoidance for Cl-poor amphiboles yet weak Mg-Cl avoidance

* Present address: Institute of Mineralogy, Petrology and Economic Geology, Tohoku University, Aoba-ku, Sendai 980-77, Japan; E-mail: hsato@mail.cc.tohoku.ac.jp

for Cl-rich amphiboles under various metamorphic Cl-bearing environments. The amphibole analyses by Morrison (1991) revealed that both ^{141}Al and A-site occupancy are systematically increased in the amphibole structure from Cl-poor to Cl-rich amphibole, and that the A-site is occupied largely by K with a positive correlation between K and Cl.

Structural refinements on Cl-rich amphiboles by Makino et al. (1993) and Oberti et al. (1993) delineate three distinct features of cation-Cl correlations. The Cl substitution results in structural (geometrical) constraints for both ^{141}Al and A-site occupancy (K and Na) and a chemical constraint for Fe^{2+} . This report describes a successively zoned amphibole developed by multiple events of hydrothermal alteration during post-magmatic processes in the Ramnes cauldron of the Oslo rift, Norway. The Ramnes amphibole provides an opportunity to examine the cation-Cl substitution model based on crystal structure considerations. We also discuss the origin of the successive zoning that traces the alteration of amphibole by multiple circulations of hydrothermal fluids.

SAMPLES

The volcano-plutonic Ramnes cauldron complex is typical of a series of peralkaline igneous complexes in the Permo-Carboniferous Oslo rift (Sørensen 1975). The Rb-Sr age of the plutonic rocks is 268 Ma (Rasmussen et al. 1988). The complex consists mainly of rhyolite, syenite, and alkali granitic rocks. Amphibole occurs only in porphyritic alkali granitic rocks in the central part of the pluton, from which rock samples (RAM-52, RAM-56, and RAM-58) were collected for this study (Fig. 1). These granitic rocks are composed mainly of plagioclase, potassium feldspar, quartz, diopsidic clinopyroxene, amphibole, and biotite. Accessory minerals are magnetite, ilmenite, apatite, zircon, titanite, and fluorite. Plagioclase and potassium feldspar are euhedral, and amphibole and biotite occur as subhedral phases. Quartz is an irregular, interstitial phase.

The granitic rocks commonly exhibit evidence of hydrothermal alteration. Clinopyroxene occurs as corroded crystals and its periphery is altered to amphibole. Primary amphibole is partly altered to form secondary amphibole zones at the margins, as described in this paper. Biotite is partly altered to chlorite. Interstitial quartz has abundant fluid inclusions containing solid phases, most of which were optically identified to be halite. The granitic rocks generally contain miarolitic cavities. These petrographic features are essentially similar to those of hydrothermally altered granitic rocks, described from peralkaline silicic intrusions in the Oslo rift, such as the Eikeren and Sande complex (Neumann et al. 1990; Hansteen et al. 1990; Andersen 1990).

ANALYTICAL METHOD

Analyses of the zoned amphibole were made using a JXA-50A electron microanalyzer with an accelerating po-

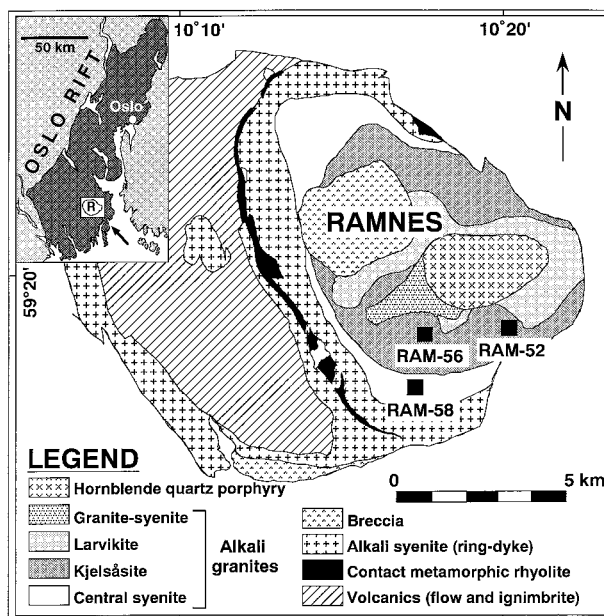


FIGURE 1. Map of the Ramnes cauldron after Sørensen (1975), showing sample locations.

tential of 15 kV. Sample current was 20 nA for major element analyses and 40 nA for chlorine and fluorine analyses. Spot analysis was carried out using the back-scattered electron image for location. The standard materials for data correction of major elements were previously described (Yamaguchi et al. 1974) and used in the former pyroxene and amphibole studies (Yamaguchi et al. 1978; Yamaguchi et al. 1983; Yamaguchi 1985; Kawakatsu and Yamaguchi 1987). The standard materials were as follows: synthetic wollastonite glass for Si and Ca, natural albite and adularia for Na and K, and synthetic TiO_2 , Al_2O_3 , Fe_2O_3 , MnO, and MgO. Synthetic fluor phlogopite was used as the reference standard for F analyses (Kawakatsu and Yamaguchi 1987), and halite was used for Cl analyses (Tsuchiya 1986; Yamaguchi 1989). The Bence and Albee (1968) matrix correction was made using alpha factors for a take-off angle of 35° calculated by the method of Albee and Ray (1970) for JEOL data correction system (XM-OFP) (Akasaka and Yamaguchi 1988), after background and dead-time corrections. To check the use of halite for Cl analysis in the course of a study on glass inclusions in volcanic phenocrysts (Yamaguchi in preparation), we have analyzed glass of Juan de Fuca Ridge basalt with 450 ppm Cl (Kohno 1992). The resultant microprobe analysis is 450 ± 30 ppm. Vanko (1986) has also reported good analytical results for Cl using halite as a standard. Intensity data were obtained using a TAP crystal for F and a PET crystal for Cl. The counting times were 60 s on peak and at each of offset background positions. Detection limits for F and Cl were about 1700 and 80 ppm, respectively.

Structural formulae of amphiboles were calculated on the basis of 23 O atoms. Values of $\text{Fe}^{3+}/(\text{Fe}^{3+} + \text{Fe}^{2+})$ of

TABLE 1. Selected spot analyses of zones amphibole in RAM-52

Spot	1	FA-1	2	3	4	5	6	7	8	9	10
Zone	FA	FA	FA	HH	FE						
Position (μm)	0	—	6	16	20	24	28	34	40	48	58
SiO ₂	47.57	44.43	45.65	38.31	38.12	38.25	38.20	39.05	39.65	39.62	41.50
TiO ₂	0.02	0.04	0.03	0.18	0.34	0.45	0.54	0.66	0.71	0.81	1.43
Al ₂ O ₃	2.95	5.04	4.28	10.07	9.97	9.97	9.94	9.60	9.19	9.50	8.01
Fe ₂ O ₃ *	4.07	5.68	4.74	4.38	5.73	5.88	5.06	5.85	5.13	5.18	5.10
FeO	28.46	28.07	28.69	27.26	25.65	24.92	24.58	23.18	23.21	22.61	20.06
MnO	0.96	0.73	0.84	0.50	0.42	0.47	0.45	0.47	0.48	0.44	0.47
MgO	1.99	0.82	1.53	1.20	1.81	2.22	2.58	3.43	3.79	4.04	5.86
CaO	10.58	10.22	10.32	10.75	10.57	10.48	10.60	10.47	10.57	10.58	10.31
Na ₂ O	0.51	0.81	1.05	1.80	1.88	1.94	1.93	1.99	1.97	2.05	2.01
K ₂ O	0.26	0.36	0.71	1.87	1.82	1.92	1.74	1.72	1.62	1.45	1.07
F	0.00	0.06	0.02	0.05	0.01	0.08	0.03	0.14	0.18	0.24	0.50
Cl	0.08	0.32	0.36	2.81	2.88	2.96	2.90	2.60	2.33	2.07	0.82
—O=F+Cl	0.02	0.10	0.09	0.66	0.65	0.70	0.67	0.65	0.60	0.57	0.40
Total	97.44	96.47	98.14	98.52	98.56	98.83	97.88	98.52	98.22	98.03	96.74
H ₂ O _{calc} **	1.86	1.73	1.77	1.07	1.08	1.03	1.06	1.11	1.17	1.21	1.43
Total _{calc}	99.31	98.21	99.91	99.59	99.64	99.86	98.94	99.64	99.39	99.25	98.17
Structural formulae based on 23 O atoms											
Si	7.568	7.221	7.303	6.335	6.277	6.270	6.293	6.333	6.416	6.388	6.599
^[4] Al	0.432	0.779	0.697	1.665	1.723	1.730	1.707	1.667	1.584	1.612	1.401
ΣT	8.000	8.000	8.000	8.000	8.000	8.000	8.000	8.000	8.000	8.000	8.000
^[6] Al	0.122	0.186	0.110	0.296	0.212	0.195	0.222	0.167	0.168	0.193	0.100
Ti	0.002	0.005	0.004	0.023	0.043	0.055	0.068	0.081	0.087	0.098	0.170
Fe ³⁺	0.487	0.695	0.571	0.545	0.711	0.725	0.627	0.714	0.625	0.629	0.610
Fe ²⁺	3.787	3.816	3.838	3.769	3.532	3.416	3.387	3.144	3.140	3.049	2.667
Mn	0.130	0.101	0.113	0.071	0.058	0.065	0.063	0.065	0.066	0.060	0.064
Mg	0.471	0.198	0.364	0.296	0.445	0.543	0.633	0.829	0.914	0.971	1.389
$\Sigma\text{M}_{1,2,3}$	5.000	5.000	5.000	5.000	5.000	5.000	5.000	5.000	5.000	5.000	5.000
Ca	1.803	1.780	1.768	1.904	1.865	1.841	1.871	1.820	1.832	1.828	1.757
^[4] Na	0.159	0.220	0.232	0.096	0.135	0.159	0.129	0.180	0.168	0.172	0.243
ΣM_4	1.962	2.000	2.000	2.000	2.000	2.000	2.000	2.000	2.000	2.000	2.000
^[6] Na	—	0.035	0.095	0.480	0.467	0.457	0.487	0.446	0.451	0.469	0.377
K	0.053	0.074	0.146	0.394	0.383	0.401	0.365	0.357	0.335	0.297	0.216
ΣA	0.053	0.109	0.241	0.874	0.850	0.858	0.852	0.803	0.786	0.767	0.594
F	0.000	0.030	0.009	0.028	0.005	0.042	0.014	0.072	0.090	0.121	0.254
Cl	0.021	0.088	0.098	0.787	0.805	0.823	0.809	0.715	0.638	0.565	0.222
OH _{calc}	1.979	1.882	1.892	1.186	1.190	1.135	1.177	1.214	1.272	1.313	1.524
ΣO_3	2.000	2.000	2.000	2.000	2.000	2.000	2.000	2.000	2.000	2.000	2.000
R ³⁺ †	0.614	0.890	0.688	0.887	1.008	1.031	0.984	1.044	0.967	1.018	1.050
X _{Fe²⁺} ‡	0.889	0.951	0.913	0.927	0.888	0.863	0.843	0.791	0.775	0.758	0.658
X _{Fe³⁺} §	0.114	0.154	0.130	0.126	0.167	0.175	0.156	0.185	0.166	0.171	0.186
Z	11.373	11.476	11.455	11.797	11.762	11.749	11.694	11.604	11.543	11.480	11.211

Notes: FA = ferro actinolite, HH = hastingsitic hornblende, FE = ferro edenite.

* Fe³⁺/Fe²⁺ calculation based on 13eCNK method (Robinson et al. 1982).

** H₂O calculation based on an assumption of $\Sigma\text{O}_3 = 2.0$ apfu.

† R³⁺ = ^[6]Al + 2Ti + Fe³⁺.

‡ X_{Fe²⁺} = Fe²⁺/(Fe²⁺ + Mg).

§ X_{Fe³⁺} = Fe³⁺/Fe_{total}.

|| Z = mean atomic number.

amphibole were estimated using the 13eCNK method described by Stout (1972) and Robinson et al. (1982). The 13eCNK scheme gives the right Fe³⁺/(Fe³⁺ + Fe²⁺) values for amphiboles with low cummingtonite component (Yamaguchi 1985). We tried to calculate the means of the structural formulae by both the 13eCNK and the 15eCNK schemes. The latter formulae are rather close to those by the 13eCNK scheme and suggest that the amphiboles contain little cummingtonite component. The structural formulae obtained for RAM-52, 56, and 58 yield a Fe³⁺/(Fe³⁺ + Fe²⁺) range of 0.03–0.26 (a mean of 0.13).

Concentration of H₂O in one amphibole separate (RAM-52, #160–200 mesh, purified to at least 98%) was analyzed by the vacuum H₂ extraction method (Suzuoki and Epstein 1976), yielding a value of 1.28 wt% of H₂O.

Reproducibility of this method was $\pm 0.1\%$ (1 sd). The H₂O weight percent value of the separated sample is dominated by the core material (core/rim ratio >80/20) and relatively comparable to the H₂O weight percent value (1.42–1.46 wt%) calculated from the structural formulae for the amphibole core (spot 10–11 in Table 1). There is no indication of an oxyhornblende component in the Ramnes amphiboles.

COMPOSITIONAL VARIATIONS AND ZONING OF RAMNES AMPHIBOLES

Generally, amphibole in the Ramnes granites is hydrothermally altered to form secondary amphibole zones or patches in the original amphibole crystals. Therefore, microprobe spot analyses vary extensively, and amphibole

TABLE 1. *Extended*

Spot	11	12	13	14	15
Zone	FE	FE	FE	FE	FE
Position (μm)	68	74	78	88	89
SiO ₂	42.76	42.56	42.81	43.48	42.78
TiO ₂	1.37	1.40	1.37	1.42	1.68
Al ₂ O ₃	7.98	8.01	7.99	7.94	7.74
Fe ₂ O ₃ *	6.24	6.12	6.89	6.57	6.37
FeO	18.37	18.34	17.60	17.72	17.78
MnO	0.46	0.42	0.44	0.45	0.42
MgO	6.87	6.88	7.12	7.34	7.36
CaO	10.17	10.16	10.17	10.17	10.26
Na ₂ O	2.14	2.18	2.07	2.17	2.15
K ₂ O	1.13	1.08	1.07	1.07	1.03
F	0.57	0.60	0.63	0.66	0.67
Cl	0.80	0.80	0.81	0.79	0.78
-O=F+Cl	0.42	0.43	0.45	0.46	0.46
Total	98.46	98.11	98.53	99.32	98.55
H ₂ O _{calc} **	1.46	1.44	1.43	1.44	1.42
Total _{calc}	99.92	99.55	99.96	100.77	99.97
Structural formulae based on 23 O atoms					
Si	6.625	6.617	6.613	6.650	6.609
^[4] Al	1.375	1.383	1.387	1.350	1.391
ΣT	8.000	8.000	8.000	8.000	8.000
^[6] Al	0.083	0.084	0.067	0.082	0.018
Ti	0.160	0.164	0.160	0.164	0.195
Fe ³⁺	0.727	0.716	0.801	0.756	0.740
Fe ²⁺	2.380	2.385	2.274	2.267	2.297
Mn	0.061	0.056	0.057	0.058	0.055
Mg	1.588	1.596	1.640	1.674	1.695
$\Sigma\text{M1,2,3}$	5.000	5.000	5.000	5.000	5.000
Ca	1.688	1.692	1.684	1.667	1.698
^[44] Na	0.312	0.308	0.316	0.333	0.302
ΣM4	2.000	2.000	2.000	2.000	2.000
^[4] Na	0.331	0.350	0.304	0.310	0.341
K	0.224	0.214	0.211	0.208	0.203
ΣA	0.555	0.563	0.515	0.518	0.545
F	0.278	0.293	0.309	0.319	0.327
Cl	0.210	0.212	0.211	0.205	0.204
OH _{calc}	1.512	1.496	1.479	1.477	1.468
ΣO3	2.000	2.000	2.000	2.000	2.000
R ³⁺ †	1.131	1.128	1.188	1.165	1.149
X _{Fe²⁺} ‡	0.600	0.599	0.581	0.575	0.575
X _{Ca²⁺} §	0.234	0.231	0.260	0.250	0.244
Z	11.137	11.138	11.130	11.110	11.127

compositions in three rock-samples (RAM-52, RAM-56, and RAM-58) show a large compositional variation in terms of ^[4]Al and Fe²⁺/(Fe²⁺ + Mg) on the classification diagram (Leake 1978) in Figure 2. The wide variation of Fe²⁺/(Fe²⁺ + Mg) probably results from the different Fe²⁺/(Fe²⁺ + Mg) of the original rocks. Amphiboles from RAM-52 have higher Fe²⁺/(Fe²⁺ + Mg) values (mostly > 0.5) than those from the other two rocks and a large ^[4]Al range, from hastingsitic hornblende to ferro-actinolite composition. In this sample, successive amphibole zones are commonly developed at the crystal margins of the original amphibole, which has a ferro-edenitic hornblende composition.

Amphibole in the RAM-52 granite typically shows successive zoning from a brown FE core, through a bluish green HH zone, to a light green FA rim. Figure 3a shows a typical back-scattered electron image of the zoned amphibole. The zonation is not typically concentric, and the zones are developed perpendicular to the *c* axis (Fig. 3a), locally with crosscut or irregular oscillatory zoning or both. The zoning is quite similar to that of the hydro-

thermally altered amphiboles from the Daito-Yokota granitoid, southwest Japan (Kawakatsu and Yamaguchi 1987). From the textural features, magmatic amphibole composition is likely preserved in the edenitic core (more than 80 vol% of the grain).

The successively zoned amphibole from RAM-52 shows a large systematic change in composition from core to rim (FE→HH→FA) within a distance of <100 μm (Fig. 3a). Twenty-two systematic spot-analyses were made on the single grain from rim to core. The resultant analyses are shown in Table 1. Mean atomic numbers calculated for the mapped points (Table 1) correspond well to the brightness of those areas in Figure 3a. Figure 4 shows a compositional profile of fifteen spots on the line in Figure 3b. Cl content strongly increases from the FE (0.78–0.82 wt%) to the HH zones (2.07–2.96 wt%) and abruptly decreases in the FA zone (0.01–0.36 wt%). In contrast, F content is very low and decreases in the HH and FA zones (Fig. 4). Cl-rich amphibole (2.96 wt%, 0.82 apfu) in the HH zone has high concentrations in both ^[4]Al (1.73 apfu) and A-site occupancy ($\Sigma\text{A} = 0.86$). The Cl-rich amphibole has the highest mean atomic numbers in the amphibole zones, on account of the high Cl and K contents in spite of low total Fe content relative to that of the FA rim amphibole. Both ^[4]Al and A-site occupancy vary systematically with positive correlations to Cl content throughout the three amphibole zones. Amphibole containing the higher Cl in the Cl-rich zone (HH) has the higher K/(K + Na) value (0.47). On the other hand, Fe²⁺ is not so simply correlated to the Cl content, with a high Fe content of the FA zone in spite of its large decrease in Cl content. The successive amphibole zones from RAM-52 show a large compositional range of ^[4]Al positively correlated with ΣA , and the cationic exchange is dominated by pargasite substitution composed of edenite and tschermakite substitutions (Fig. 5).

EFFECTS OF ^[4]AL, K, AND Fe²⁺ SUBSTITUTIONS FOR CHLORINE INCORPORATION

In previous studies of Cl-rich amphibole, positive correlations of ^[4]Al and ΣA with Cl content have been described (Ito and Anderson 1983; Vanko 1986; Suwa et al. 1987; Morrison 1991; Enami et al. 1992). Suwa et al. (1987) and Morrison (1991) pointed out that substitution of K in the A site effectively influences the incorporation of Cl. On the effects of Fe in octahedral sites, Vanko (1986) suggested that structural controls are not effective between Cl incorporation and Fe substitution into the octahedral site. The amphibole analyses from the ocean-floor metamorphic rocks of the Mathematician Ridge showed that Cl content of amphibole is a function of the Cl activity of the hydrothermal fluid (Vanko 1986).

Crystal-structure refinements of Cl amphiboles reveal large effects of cationic substitutions on Cl incorporation (Makino et al. 1993; Oberti et al. 1993), as follows: (1) The incorporation of Cl into the O3 site expands the octahedral strips of amphiboles, and the double chain is deformed to fit the expanded octahedral strips. This is

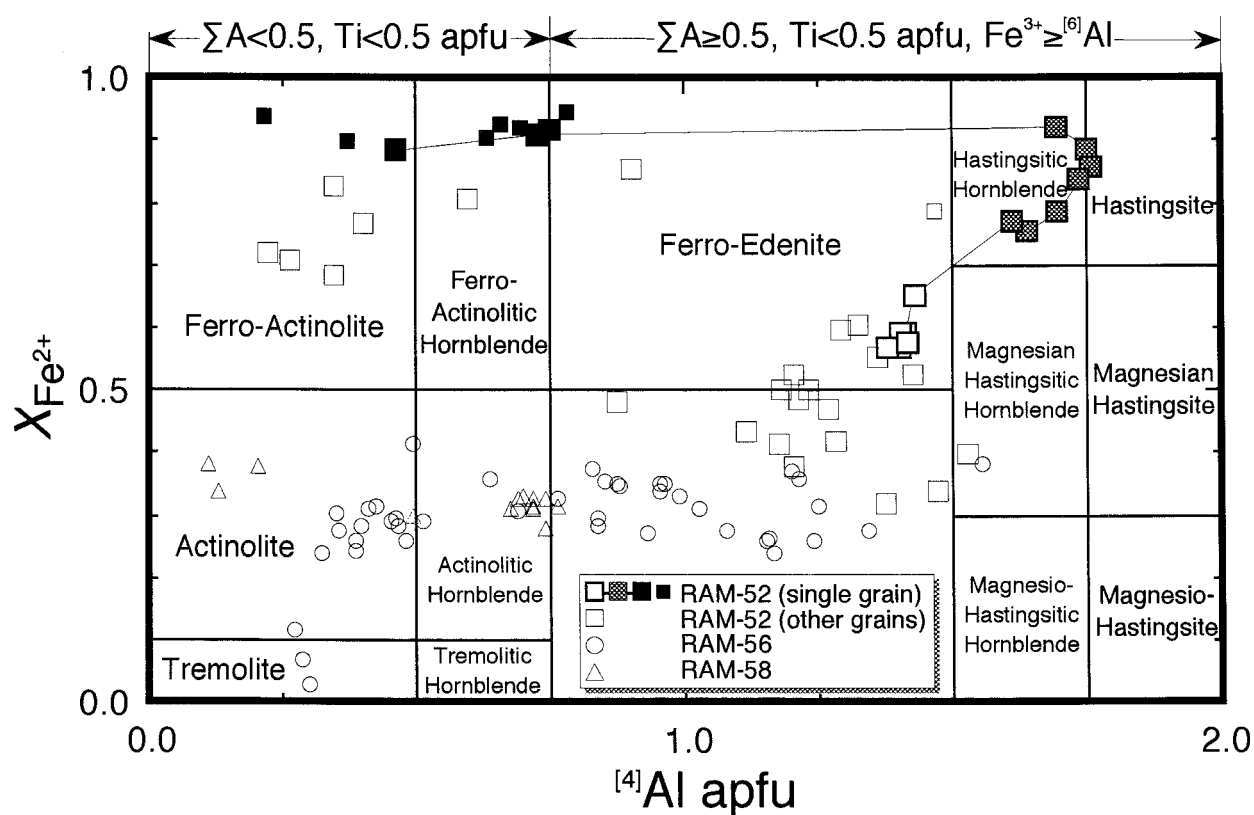


FIGURE 2. Amphibole compositions plotted in Leake's (1978) classification diagram. The zoned amphibole in RAM-52 varies in large compositional range from core to rim in a sequence of ferro-edenite (FE) core→hastingsitic hornblende zone (HH)→ferro-actinolite rim (FA). Amphiboles in RAM-56 plot in edenite-actinolitic hornblende-actinolite area, and those in RAM-58 are in actinolitic hornblende-actinolite area.

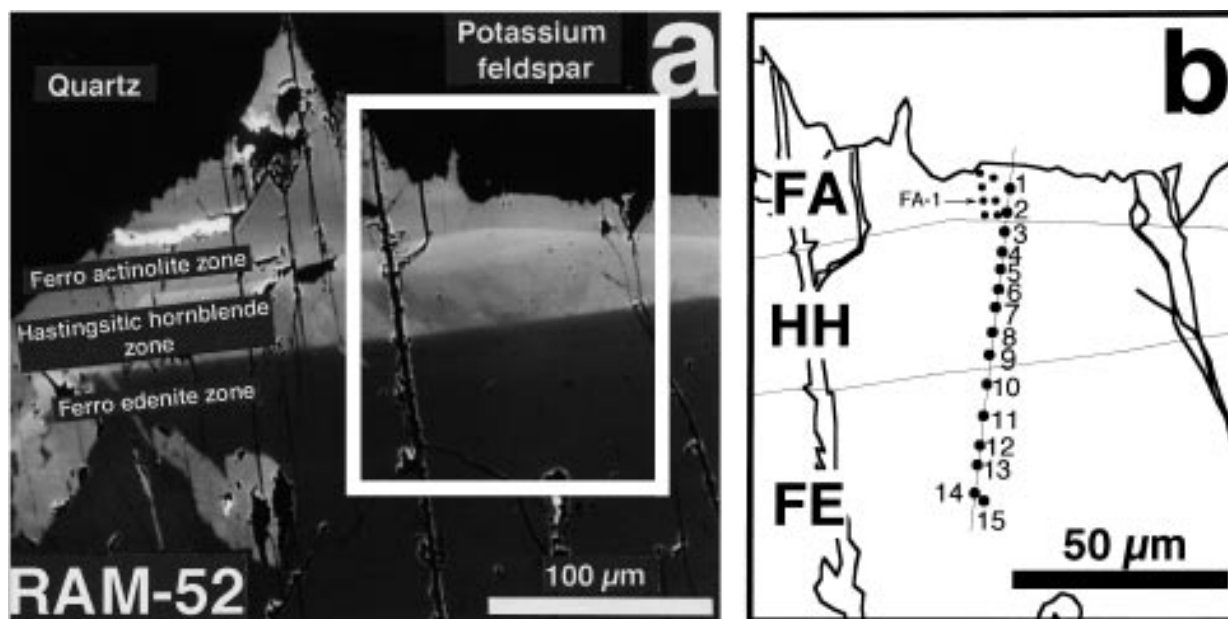


FIGURE 3. (a) Back-scattered electron scanning image of the zoned amphibole grain (RAM-52). The amphibole zones are divided into three zones (FE: ferro edenite core; HH: hastingsitic hornblende zone; FE: ferro actinolite rim). (b) Analytical points. The numbered points represent the spot analyses shown in Table 1. The points (1→15) on a line represent the trace of the step analysis shown in Figure 4.

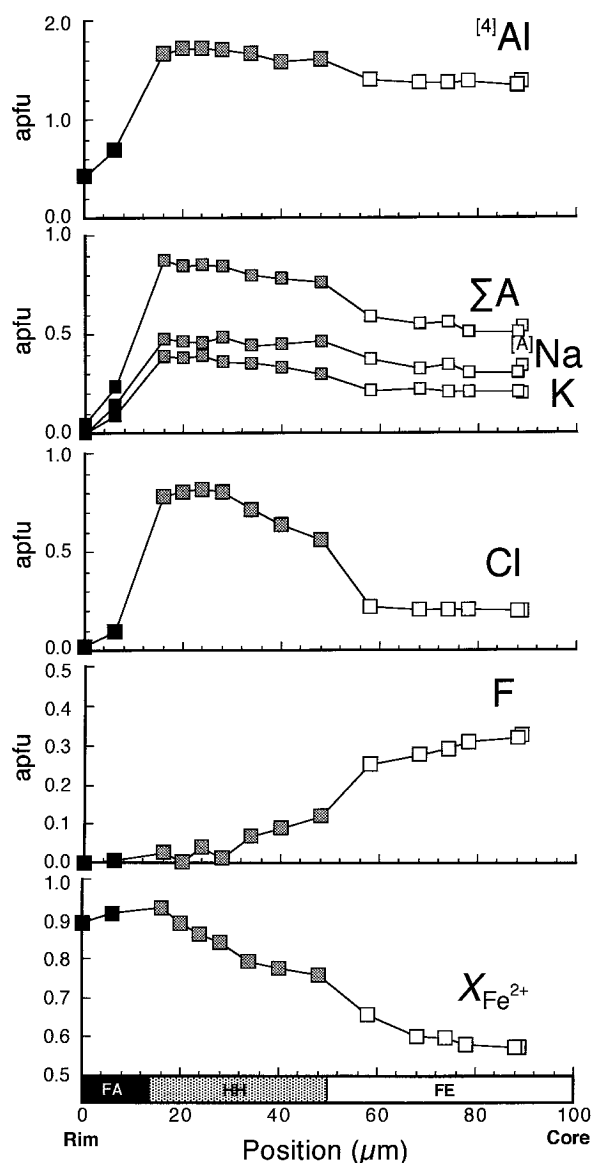


FIGURE 4. Compositional profiles of the zoned amphibole in RAM-52. Analytical points are shown in Figure 3b. See text.

achieved largely by Al substitution for Si (geometrical constraint). (2) The Cl anion projects toward the large A cavity and may be bonded to large cations in the A site. Therefore, a fully occupied A site is more stable electrostatically than a vacant A in Cl amphiboles (A-site constraint). The A site of Cl amphiboles is a better fit dimensionally for a large K cation rather than Na, and thus K is preferred in the A site. (3) The strong preference of Fe^{2+} for the M1 and M3 against the M2 was observed in the Cl amphiboles, in comparison with Cl-free amphiboles. This observation implies that Mg-Cl avoidance is realized in the intracrystalline exchange reaction among these octahedral sites of the Cl amphiboles, because Cl in O3 site is bonded to the M1 and M3 sites but not to

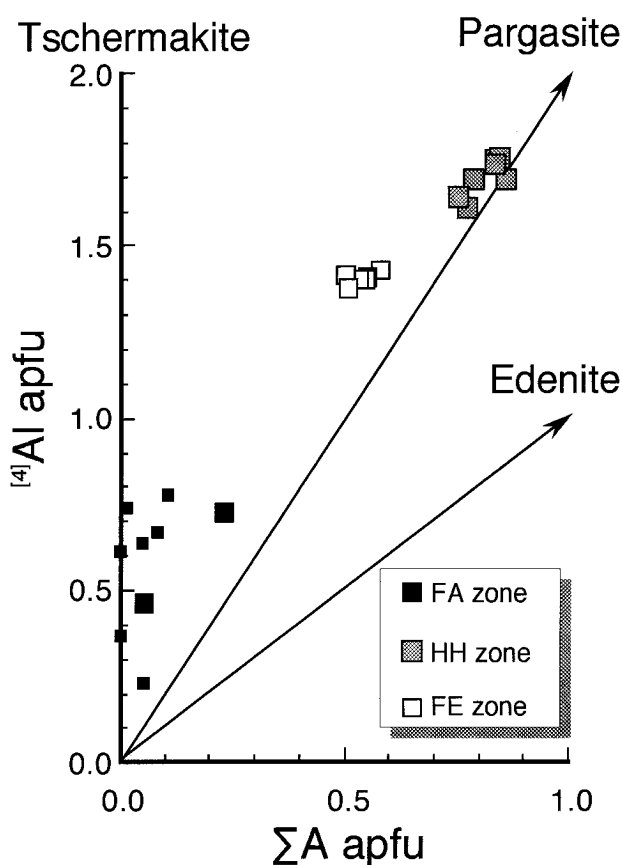


FIGURE 5. Plots of $^{[4]}\text{Al}$ vs. ΣA of the zoned amphibole from RAM-52. ΣA is positively correlated with $^{[4]}\text{Al}$, and the cationic substitution is dominated by the pargasite substitution composed of the edenite and tschermakite substitutions.

the M2 site. The significant expansion of the octahedral strips is caused mainly by substitution of the large Cl anion for OH and the effect of the Mg- Fe^{2+} substitution is little. Thus, the short range order of Fe^{2+} -Cl is not simply interpreted by geometrical consideration but may be a chemical effect (chemical constraint). Therefore, there is not large structural control on the effects of Fe substitution into octahedral sites for the Cl incorporation in amphibole, as emphasized by Vanko (1986).

These three constraints simultaneously should control the substitution of OH by Cl in the amphibole structure. Both the geometrical and A-site constraints require the enrichment of pargasite or edenite components for Cl incorporation in amphiboles, and the Fe^{2+} content may be affected by the chemical constraint. The overall effects on the Cl incorporation in amphiboles could be expressed tentatively by the product of the geometrical constraint (pargasite, tschermakite, or edenite substitution) and the chemical constraint (Fe^{2+} content). In the Ramnes Cl amphibole, there is a linear correlation between $^{[4]}\text{Al}$ and ΣA (Fig. 5), and $^{[4]}\text{Al}$ can be chosen as a parameter of the

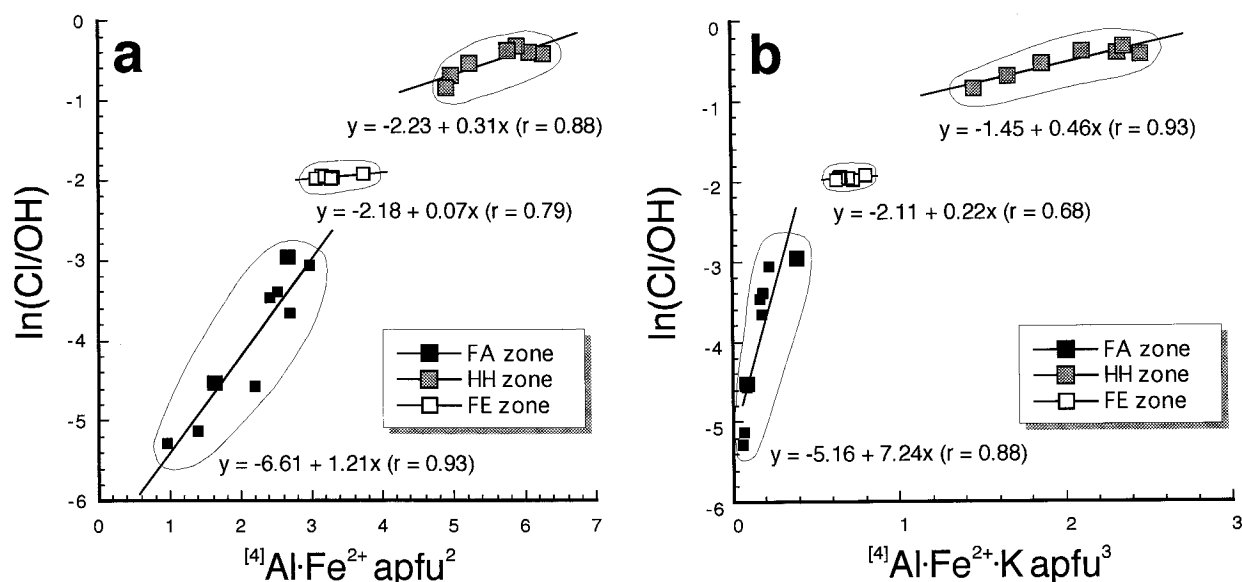


FIGURE 6. Compositional plots of amphibole for the three distinct zones (FE, HH, and FA) from RAM-52. (a) $^{[4]}\text{Al}\cdot\text{Fe}^{2+}$ vs. $\ln(\text{Cl}/\text{OH})$ plots and (b) $^{[4]}\text{Al}\cdot\text{Fe}^{2+}\cdot\text{K}$ vs. $\ln(\text{Cl}/\text{OH})$.

pargasite substitution. The Cl-OH exchange reaction of amphibole with fluid (or melt) is written as follows:



The Cl distribution may be ideally expressed by

$$\ln(\text{Cl}/\text{H})_{\text{amp}} = \ln(\text{Cl}/\text{OH})_{\text{fluid}} - \Delta G^0/RT \quad (2)$$

where ΔG^0 is the free energy changes of the end-members in the reaction (1), R and T are ideal gas constant and temperature, respectively. Obviously, the ΔG^0 varies with the cation contents in amphibole. The ΔG^0 may depend on the product of the $^{[4]}\text{Al}$ and Fe^{2+} content in the zoned amphibole (RAM-52), based on the above consideration. Using a simple function as the first approximation, Equation 2 may be rewritten as:

$$\ln(\text{Cl}/\text{OH})_{\text{amp}} = \ln(\text{Cl}/\text{OH})_{\text{fluid}} + A \cdot ^{[4]}\text{Al}\cdot\text{Fe}^{2+}/RT + B/RT \quad (3)$$

where A and B are constants.

Figure 6a shows $^{[4]}\text{Al}\cdot\text{Fe}^{2+}$ vs. $\ln(\text{Cl}/\text{OH})$ as distinct linear trends for each amphibole zone (FE, HH, and FA zone) of RAM-52. The linear relationships substantiate that the Cl incorporation in amphibole is affected by the geometrical and chemical constraints. Because the $^{[4]}\text{Al}$ content is here a parameter of the pargasite substitution, the ferropargasite component in the zoned amphibole plays the most important role for accommodating Cl in amphiboles. Further, the K content shows a strong correlation with the Cl content in the zoned amphibole (Fig. 4). To examine the effect of K incorporation in the A site, $^{[4]}\text{Al}\cdot\text{Fe}^{2+}\cdot\text{K}$ vs. $\ln(\text{Cl}/\text{OH})$ is illustrated in Figure 6b. The amphibole compositions in the three distinct zones are more clearly defined in this plot. Therefore, K is strongly

preferred in the A site of the Cl-rich amphiboles. The Cl-K bonding may be important, as expected from the above crystal structure considerations; however the value of K in the A site is not so clearly verified a parameter as the $^{[4]}\text{Al}$ and Fe^{2+} are in the above substitution in the Ramnes amphibole.

SUCCESSIVE ZONING AND HYDROTHERMAL ALTERATION

Melt-mineral-fluid interaction studies have revealed that a highly saline hydrothermal fluid was evolved during the solidification of peralkaline silicic intrusions in the Oslo rift (Neumann et al. 1990; Hansteen and Burke 1990; Andersen 1990). Early hydrothermal fluids exsolved from magma carried large amount of dissolved salts, and then a low-temperature and low-saline fluid was produced probably through dilution by mixing with meteoric water (Hansteen and Burke 1990). Extensive hydrothermal alteration of mafic silicates and the common occurrence of halite-bearing fluid inclusions in anhedral quartz suggest that hydrothermal fluids were exsolved from semi-solidified magma at near solidus conditions of the Ramnes alkali granite magma.

Three distinct trends in the $^{[4]}\text{Al}\cdot\text{Fe}^{2+}$ vs. $\ln(\text{Cl}/\text{OH})$ and the $^{[4]}\text{Al}\cdot\text{Fe}^{2+}\cdot\text{K}$ vs. $\ln(\text{Cl}/\text{OH})$ plots for the amphibole zones (FE, HH, and FA in Figs. 6a and 6b) likely indicate magmatic conditions followed by corrosion and growth because of different conditions in chemistry and temperature of coexisting hydrothermal fluids. The distinction of the three zones in these plots is related to the pattern of the Fe zoning profile (Fig. 4). The Cl content of amphibole does not vary as a function of Fe substitution in the FA zone, and it is suggested that this outer

high Fe/Cl edge was formed by a relatively high Fe/(Fe + Mg) hydrothermal fluid, in comparison with the inner, HH zone. This hydrothermal fluid could also have been at lower temperature than the fluid that produced the inner, HH zone, because the compositional trend of the outer high Fe/Cl edge (FA rim) has a relatively steeper gradient in the $\ln(\text{Cl}/\text{OH})$ plots (Figs. 6a and 6b).

The successive zoning of amphibole was developed through two stages of hydrothermal alteration of the original magmatic (FE) hornblende. The considerations discussed suggest that, in the early hydrothermal event, a relatively high-temperature and high-saline fluid altered the original FE to the Cl-rich HH at the crystal margins adjacent to circulating fluids. Late-stage hydrothermal alteration by a high Fe/Cl and low-temperature fluid produced FA at the crystal edges. This late stage alteration may have been more extensive than the early one because it is commonly for the FA to cut across or replace the early HH zone. Thus, each amphibole zone typically developed on corroded, uncomformable surfaces.

ACKNOWLEDGMENTS

We gratefully acknowledge the cooperation of M. Ohta of Norsk Polar Institute, Y. Kuroda and T. Yamada of Shinshu University, and S. Kanisawa and S. Kojima of Tohoku University. We thank J.H. Berg, D.A. Vanko, J. Morrison, and R.J. Swope for their helpful and critical reviews of the manuscript. Their comments were of great importance for this publication. This research was supported by a Grant-in Aid for Scientific Research to Y. Kuroda from the Ministry of Education, Science, and Culture of Japan (63041063).

REFERENCES CITED

- Akasaka, M., and Yamaguchi, Y. (1988) Improvement of EPMA correction computer program for off-line quantitative analysis. Geological Report of Shimane University, 7, 85–90 (in Japanese).
- Albee, A.L., and Ray, L. (1970) Correction factors for electron probe microanalysis of silicates, oxides, carbonates, phosphates and sulfates. *Analytical Chemistry*, 42, 1408–1411.
- Andersen, T. (1990) Melt-mineral-fluid interaction in peralkaline silicic intrusions in the Oslo Rift, southeast Norway. IV: Fluid inclusions in the Sande nordmarkite. *Norges Geologiske Undersøkelse*, 417, 41–54.
- Bence, A.E., and Albee, A.L. (1968) Empirical correction factors for the electron-microanalysis of silicates and oxides. *Journal of Geology*, 76, 382–403.
- Burnham, C.W., and Ohmoto H. (1980) Late-stage processes of felsic magmatism. *Mining Geology Special Issue*, 8, 1–11.
- Chivas, A.R. (1981) Geochemical evidence for magmatic fluids in porphyry copper mineralization. *Contribution to Mineralogy and Petrology*, 78, 389–403.
- Dick, L.A., and Robinson, G.W. (1979) Chlorine-bearing potassic hastingsite from a sphalerite skarn in southern Yukon. *Canadian Mineralogist*, 17, 25–26.
- Enami, M., Liou, J., and Bird, D.K. (1992) Cl-bearing amphibole in the Salton Sea geothermal system, California. *Canadian Mineralogist*, 30, 1077–1092.
- Hansteen, T.H., and Burke, A.J. (1990) Melt-mineral-fluid interaction in peralkaline silicic intrusions in the Oslo Rift, southeast Norway. II: High-temperature fluid inclusions in the Eikeren-Skrim complex. *Norges Geologiske Undersøkelse*, 417, 15–32.
- Ito, E., and Anderson, A.T., Jr. (1983) Submarine metamorphism of gabbros from the Mid-Cayman Rise: Petrographic and mineralogic constraints on hydrothermal processes at slow-spreading ridges. *Contribution to Mineralogy and Petrology*, 82, 371–388.
- Kawakatsu, K., and Yamaguchi, Y. (1987) Successive zoning of amphiboles during progressive oxidation in the Daito-Yokota granitic complex, San-in belt, southwest Japan. *Geochimica et Cosmochimica Acta*, 51, 535–540.
- Kilinc, I. A., and Burnham, C. W. (1972) Partitioning of chloride between a silicate melt and coexisting aqueous phase from 2 to 8 kilobars. *Economic Geology*, 67, 231–235.
- Kohno, M.K. (1992) Emission of sulfur, chlorine and fluorine to the atmosphere by volcanic eruptions in Japan in the last 1300 years, 53 p. M.S. thesis, Institute for Study of the Earth's Interior, Okayama University, Japan.
- Leake, B.E. (1978) Nomenclature of amphibole. *American Mineralogist*, 63, 1023–1052.
- Makino, K., Tomita, K., and Suwa, K. (1993) Effect of chlorine on the crystal structure of a chlorine-rich hastingsite. *Mineralogical Magazine*, 57, 677–685.
- Morrison, J. (1991) Compositional constraints on the incorporation of Cl into amphiboles. *American Mineralogist*, 76, 1920–1930.
- Munoz, J.L. (1984) F-OH and Cl-OH exchange in micas with applications to hydrothermal ore deposits. In *Micas. Reviews in Mineralogy*, 13, 469–493.
- Nedachi, M. (1980) Chlorine and fluorine contents of rock-forming minerals of the Neogene granitic rocks in Kyushu, Japan. *Mining Geology Special Issue*, 8, 39–48.
- Neumann, E.-R., Andersen, T., and Hansteen, T.H. (1990) Melt-mineral-fluid interaction in peralkaline silicic intrusions in the Oslo Rift, south-east Norway. I: Distribution of elements in the Eikeren ekerite. *Norges Geologiske Undersøkelse*, 417, 1–13.
- Oberti, R., Ungaretti, L., Cannillo, E., and Hawthorne, F.C. (1993) The mechanism of Cl incorporation in amphibole. *American Mineralogist*, 78, 746–752.
- Rasmussen, E., Neumann, E.-R., Andersen, T., Sundvoll, B., Fjerdingsstad, V., and Stabel, A. (1988) Petrogenetic processes associated with intermediate and silicic magmatism in the Oslo rift, south-east Norway. *Mineralogical Magazine*, 52, 293–307.
- Robinson, P., Spear, F.S., Schumacher, J.C., Laird, J., Klein, C., Evans, B.W., and Doolan, B.L. (1982) In *Mineralogical Society of America, Reviews in Mineralogy*, 9B, p. 1–227.
- Shinohara, H., Iiyama, J. T., and Matsuo, S. (1989) Partition of chlorine compounds between silicate melt and hydrothermal solutions: I. Partition of NaCl-KCl. *Geochimica et Cosmochimica Acta*, 53, 2617–2630.
- Stout, J.H. (1972) Phase petrology and mineral chemistry of coexisting calcic amphiboles from Telemark, Norway. *Journal of Petrology*, 13, 99–145.
- Suwa, K., Enami, M., and Horiuchi, T. (1987) Chlorine-rich potassium hastingsite from West Ongul Island, Lützow-Holm Bay, East Antarctica. *Mineralogical Magazine*, 51, 709–714.
- Suzuoki, T., and Epstein, S. (1976) Hydrogen isotope fractionation between OH-bearing minerals and water. *Geochimica et Cosmochimica Acta*, 40, 1229–1240.
- Sørensen, R. (1975) The Ramnes cauldron in the Permian of the Oslo region, southern Norway. *Norges geologiske undersøkelse*, 321, 67–86.
- Tsuchiya, N. (1986) Cl and F contents of apatite in the Matsumae plutonic rocks, southwestern Hokkaido, Japan—A useful indicator of vapor saturation. *Journal of Japan Association of Mineralogy, Petrology and Economic Geology*, 81, 67–76.
- Vanko, D.A. (1986) High-chlorine amphiboles from oceanic rocks: Product of highly saline hydrothermal fluids. *American Mineralogist*, 71, 51–59.
- Volfinger, M., Robert, J.L., Vielzeuf, D., and Neiva, A.M.R. (1985) Structural control of the chlorine content of OH-bearing silicates (micas and amphiboles). *Geochimica et Cosmochimica Acta*, 49, 37–48.
- Yamaguchi, Y. (1985) Hornblende-cummingtonite and hornblende-actinolite intergrowths from the Koyama calcalkaline intrusion, Susa, southwest Japan. *American Mineralogist*, 70, 980–986.
- (1989) F and Cl contents of hornblende-actinolite from metagabbros in Ashidachi area of the Sangun belt, southwest Japan. *Memoir of Geological Society of Japan*, 33, 81–88 (in Japanese).
- Yamaguchi, Y., Tomita, K., and Sawada, Y. (1974) Crystallization trend

- of zoned pyroxenes in quartz gabbro from the Koyama intrusive complex at Mt. Koyama, Yamaguchi prefecture, Japan. *Memoirs of the Geological Society of Japan*, 11, 69–82.
- Yamaguchi, Y., Tomita, K., and Akai, J. (1978) Clinoamphibole lamellae in diopside of garnet lherzolite from Alpe Arami, Bellinzona, Switzerland. *Contribution to Mineralogy and Petrology*, 66, 263–270.
- Yamaguchi, Y., Shibakusa, H., and Tomita, K. (1983) Exsolution of cumingtonite, actinolite and sodic amphibole in hornblende in high-pressure metamorphism. *Nature*, 304, 257–259.

MANUSCRIPT RECEIVED SEPTEMBER 12, 1995

MANUSCRIPT ACCEPTED DECEMBER 20, 1996